coatings

MDPI

Article

Sol-Gel SiO_2 Coatings with Curcumin and Thymol on 3D Printouts Manufactured from Ti6Al4V ELI

Natalia Słabęcka, Karolina Czajkowska, Paulina Łataś, Patryk Śniarowski, Laura Ciosek, Krzysztof Jastrzębski and Bożena Pietrzyk *

Institute of Materials Science and Engineering, Faculty of Mechanical Engineering, Lodz University of Technology, Stefanowskiego 1/15, 90-537 Lodz, Poland; nataliaslabecka@gmail.com (N.S.); kczajkowska2701@gmail.com (K.C.); paulinalatas7@gmail.com (P.Ł.); patryk.sniarowski@wp.pl (P.Ś.); laura.ciosek@tlen.pl (L.C.); krzysztof.jastrzebski@p.lodz.pl (K.J.)
* Correspondence: bozena.pietrzyk@p.lodz.pl

Abstract: Bacterial biofilm on implants may cause inflammation, which disturbs the process of the implant's integration with the surrounding tissues. Such problems are becoming critical for patients' health, especially in connection with the presence of antibiotic-resistant bacterial strains. Among the existing alternatives for drug treatments are natural-based substances. This study focused on the examination of silica coatings with curcumin and thymol, which were deposited using the sol-gel method on 3D printouts made of Ti6Al4V ELI. This substrate material is commonly used in medicine. The selective laser melting technique used for the manufacturing of samples was in line with the existing procedures applied for individual orthopedic implants. The examination involved the assessment of the coatings' morphology, chemical composition, and biological effect. The antibacterial properties were tested using a flow cytometer using *Escherichia coli*, and the cytotoxicity on Saos-2 cells was assessed using the LIVE/DEAD test. The obtained results showed that it is possible to produce silica sol-gel coatings with the addition of specific natural substances in concentrations assuring a bacteriostatic effect. The produced coatings did not show any cytotoxic effect, which confirms the possibility of using both curcumin and thymol as additives to coatings used in medicine, e.g., for orthopedic implants.

Keywords: sol-gel coatings; natural antibacterials agents; curcumin; thymol; 3D printing

check for updates

Citation: Słabęcka, N.; Czajkowska, K.; Łataś, P.; Śniarowski, P.; Ciosek, L.; Jastrzębski, K.; Pietrzyk, B. Sol-Gel SiO_2 Coatings with Curcumin and Thymol on 3D Printouts Manufactured from Ti6Al4V ELI. *Coatings* **2024**, *14*, 1149. https://doi.org/10.3390/coatings14091149

Academic Editor: Oana Dragos-Pinzaru

Received: 18 July 2024
Revised: 2 September 2024
Accepted: 3 September 2024
Published: 6 September 2024

Copyright: © 2024 by the authors. Licensee MDPI, Basel, Switzerland. This article is an open access article distributed under the terms and conditions of the Creative Commons Attribution (CC BY) license (https://creativecommons.org/licenses/by/4.0/).

1. Introduction

Antibiotics, in their almost one hundred years of conscious usage, have become an integral part of medicine. However, their excessive use (both as medical therapeutic sand in the food industry) has resulted in a more frequent occurrence of microorganisms resistant to their effects and causes problems with the treatment of patients exposed to action of those microbes. The problem of antibiotic resistance has been recognized by the WHO as a key threat to public health, affecting all countries regardless of their level of development [1]. The limited capability to straightforwardly fight infection takes humanity back to the beginning of the 20th century and has resulted in a rising number of medical complications and even the deaths of patients due to antibiotic-resistant microorganisms. In addition, there are also economic aspects of antibiotic resistance, including increasing costs of care and an extended length of hospitalization [1,2].

Approximately 60%–70% of antibiotics have poor permeability resulting from their insufficient intracellular retention, which means that these substances are not effective enough for any type of infection [3]. In addition, microorganisms have developed mechanisms to cope with the detrimental effects of antibiotics, such as cell wall synthesis, DNA replication, and protein translation machinery. Resistance mechanisms cover various approaches from the expression of enzymes that are capable of degrading, modifying, or inactivating given antibiotics, to changing the cell wall composition or the activity of ion pumps, or to directly

influencing regions most susceptible to antibiotic attack, for example by post-translational modification [4].

Among the most dangerous bacterial species under the careful attention of medical doctors are methicillin-resistant *Staphylococcus aureus* (MRSA) [5–10] and cephalosporin-resistant *E. coli* [11–13]. According to the 2019 Antibiotic Resistance Report, over 2.8 million infections with antibiotic-resistant bacteria occur each year in the USA, resulting in over 35,000 deaths [14].

Among the difficult-to-treat infections are those related to the inhabitation of the surface of implants with microbes and the formation of biofilms. When bacteria attach to a given surface using adhesion proteins, they begin to not only multiply on it but also produce exopolysaccharides. This film protects them against external factors, e.g., antibiotics, and creates a firmer attachment to the surface. If peri-implant infection occurs, the osseointegration process may be impaired. Bacterial infection causes inflammation, which initiates the process of bone tissue resorption around the implant. This further leads to the loosening of the implant as a result of micro-movements. Peri-implant infections may also cause systemic infections, which prolong hospitalization and contribute to the length of the patient's recovery [5].

One of the alternatives to antibiotics is nanoparticles, or metal ions such as silver, zinc, copper, gold, and iron [15]. However, their safety regarding human cells and the natural environment is increasingly being questioned [16–18]. Research shows that nanoparticles can accumulate in mammalian cells and have a toxic effect on them. However, the cellular response strongly depends on the shape, size, and surface properties of metal ions and nanoparticles [16,17]. Due to their dimensions, nanoparticles can enter the circulatory system and even penetrate the blood–brain barrier [16]. The common usage of products with metal nanoparticles obviously results in their release into the natural environment, resulting in further interactions with eukaryotic and prokaryotic cells [18]. Additionally, the widespread use of silver compounds as antibacterial agents has caused bacteria to develop resistance to silver [19].

The risk associated with the excessive use of antibiotics and nanoparticles as antibacterial agents motivates the search for alternative solutions that prevent bacterial infections. One of the possible solutions is the use of enzymes like lysozyme (N-acetyl-muramin hydrolase, also known as muramidase). The antibacterial effect of this naturally occurring compound is multidirectional: it causes the breakdown of polysaccharides in cell walls and disrupts the quorum-sensing systems [20]. Among the artificially synthetized compounds is parylene F, which shows antibacterial and anti-adhesive properties against Gram-negative bacteria [21].

A common approach is introducing protective antimicrobial coatings. These act on the basis of releasing active substances, e.g., metal ions, nanoparticles, chemical compounds, etc., killing microbes on contact, for example, in the case of chitosan or synthetic cationic polymers [22,23]. An interesting solution is the use of galvanic coatings produced using plasma-assisted implantation or electrospraying [24,25]. The potential difference in the metal constituents of such a coating causes the creation of electric microcells in the physiological solution, affecting bacterial health. In this case, there is no threat of gradual washing out of the antibacterial substance from such a coating [26]. More traditional approaches involve doped diamond-like carbon coatings [27] or silica sol-gel coatings with additives [28]. Sol-gel coatings in particular can be easily applied to elements of even complex shapes. The coating matrix (silica) itself does not have a bactericidal effect and is safe for human tissues, but the released substances may have a detrimental effect on bacteria [28].

Among the natural antibacterial substances, the most frequently discussed are turmeric, thyme, and oregano. The action of such a group of substances can be both active and passive. First, their action may be related to affecting the bacterial cell membrane or block metabolic processes. On the other hand, their passive effect results from the modification of environmental conditions or surface properties. They make it difficult for microorganisms to adhere or reproduce, e.g., due to changing the pH. A positive aspect of using natural

substances is related to their synergistic effects with other drugs [29,30]. Natural substances can be used directly, in the form of oils or extracts, and their key active ingredients can be isolated from them [29,30]. Regarding curcumin (found in turmeric), it does not directly kill bacteria but rather inhibits the biofilm formation and prevents microbial adhesion via affecting the quorum-sensing systems [31]. Thymol, present in thyme, causes destabilization of the bacterial cell membrane. Small thymol molecules cross the lipid barrier, leading to changes in the conformation and activity of the internal and membrane proteins of bacteria. Thymol has a biofilm-reducing effect in the case of infections such as *Escherichia coli*, *Listeria monocytogenes*, *Pseudomonas putida*, *Staphylococcus aureus* and even methicillin-resistant *Staphylococcus aureus* [32,33]. The use of natural substances is also potentially safer for organisms and the natural environment, which makes them promising candidates as antibacterial additives for coatings.

The following paper focuses on the evaluation of the antibacterial potential of SiO_2 coatings manufactured by the sol-gel method on 3D-printed surfaces obtained via the selective laser sintering (SLS) technique. The antibacterial effect was exerted by the use of the natural compounds curcumin and thymol. The metal substrate (Ti6Al4V ELI) and printing technique (SLS) were aligned for direct application in printouts used for personalized orthopedical implants.

2. Materials and Methods

2.1. Substrate Material

Titanium alloy Ti6Al4V ELI samples in the shape of cylinders (Figure 1) with a diameter of 16 mm and a height of 4 mm, manufactured by Medgal Ltd. (Białystok, Poland), were used as the substrate for sol-gel coatings. For this purpose, a ProX 320 A printer (3D Systems Corporation, Rock Hill SC, USA) was used, equipped with a working platform with dimensions of 250 × 250 mm. Printouts with an accuracy of ±0.2% were obtained using a laser power of 500 W. In order to remove the stresses resulting from the printing process, the samples were heat-treated in a high-vacuum oven before being detached from the substrate. The samples were made from powder for which 95% of the average grain size was in the range of 28–36 μm, and the maximum size did not exceed 40 μm. Samples made of Ti6Al4V rod cut to the same dimensions as mentioned above were mechanically ground, polished to a mirror-like state, and used as reference samples for the morphology examination. For the evaluation of the coatings' thickness, monocrystalline silicon wafers (100) were used as substrates.



Figure 1. Ti6Al4V ELI titanium alloy substrate prepared using the SLS method.

2.2. Coatings

2.2.1. Sol Preparation

The SiO_2 sol was prepared by mixing 5 mL of tetraethoxysilane (TEOS) (Aldrich, Steinheim Germany), 2 mL of 36% hydrochloric acid (Chempur, Piekary Śląskie, Poland), and 50 mL of ethanol (Chempur, Piekary Śląskie, Poland). The sol was stirred using a magnetic stirrer for approximately 2 h and left for 24 h before coating deposition. The

sol with 0.25% (*w*/*v*) curcumin (Sigma-Aldrich, St. Louis, MO, USA) and with 3% (*w*/*v*) thymol (Warchem S.A., Zakręt, Poland) was prepared by adding an appropriate amount of the natural agent to the measured volume of sol and stirring it for at least 10 min until fully dissolved in the sol. The choice of curcumin and thymol concentrations was based on studies by other researchers, where materials with these substances were tested in terms of antibacterial activity [31,32,34,35]. Raduly et al. tested antibacterial properties of siloxane host matrices with 0.27% curcumin dyes [34]. Irizar et al. tested bio-based hybrid nanocomposites for stone conservation and for this purpose examined the addition of 3% thymol and 3% thymol-SiO_2 mesoporous nanoparticles [35].

2.2.2. Coating Deposition

Before the deposition of coatings, substrate materials were cleaned in a series of sonicated baths. First they were cleaned in tap water with a small amount of detergent for 3 min, then with distilled water for 1 min, and finally in acetone for 3 min. A laboratory dip-coater, model TLO 0.1 (MTI Corporation, Richmond, CA, USA), was used for the deposition of coatings. The coatings were applied by immersing the substrate in a given sol and withdrawing it at a constant speed of 0.5 mm/s. After deposition, samples were left for 96 h at room temperature to allow the coatings to develop their final mechanical properties.

2.2.3. Sample Marking

The samples are abbreviated in the following manner: Ti—substrate without coating, Si—substrate with SiO_2 coating, Cur—substrate with SiO_2 coating and 0.25% curcumin, Tym—substrate with SiO_2 coating and 3% thymol. Mirror-polished Ti6Al4V was used for better visualization of coatings in the microscopic examination. To easily distinguish the samples, "3D printed" or "polished" was added to each abbreviation.

2.3. Microscopic Examination

Coating morphologies were assessed using a VHX950F (Keyence, Mechelen, Belgium) digital microscope via comparison with uncoated samples. Surface analysis was performed at 100× and 300× magnification. Further observations were performed with the use of the scanning electron microscopy (SEM) technique with a JSM-6610LV microscope (JEOL, Tokyo Japan). Observations were made using the secondary electron mode at an accelerating voltage of 20 kV. Additionally, energy-dispersive X-ray spectroscopy (EDS) was used for the verification of the chemical composition of the coatings. This study was performed in 2 repetitions.

2.4. Surface Roughness and Thickness of Coatings

The evaluation of the surface roughness was performed with the use of an optical profilometer (Sensofar, Barcelona, Metrology, Spain) on samples before and after the coating deposition. The arithmetic deviation from the mean line (Ra) and the highest roughness height (Rz) in the tested regions were determined. This study was performed in 2 repetitions. The thicknesses of coatings deposited on silicon substrates were determined with use of a reflectance spectrometer (Thin Film Analyzer UV20, Filmetrics, San Diego, CA, USA).

2.5. Assessment of Antibacterial Properties

Flow cytometry was used to assess the samples' antibacterial properties. The test was performed using a suspension of *Escherichia coli* O157:H7 (ATCC® 43890) with a density of 2×10^7 CFU/mL. On four 3D-printed samples (Ti, Si, Cur, Tym), 20 µL of bacterial suspension was applied and left for two different time intervals: 10 or 60 min. After the given exposure time, the suspension was collected from the examined surfaces and mixed with 2 µL of LIVE/DEAD kit and 200 µL of PBS buffer. The positive and negative controls were prepared in a similar manner but with 20 µL of untreated *E. coli* suspension. To kill the bacteria (positive control), an additional 20 µL of ethyl alcohol was added. This study was performed in 2 repetitions.

For visualization, the results are presented in graphs as mean ± standard deviation. Additionally, a one-way ANOVA test with a significance level of $p < 0.05$ was used for the statistical verification of the data set.

2.6. Assessment of Cytotoxicity

The cytotoxicity test using the LIVE/DEAD method was carried out in accordance with standard [36]. Bone-forming osteoblast cells, Saos-2 line cultured in consecutive McCoy's medium (with 15% of fetal bovine serum), were used for this examination. Four 3D printed samples (Ti, Si, Cur, Tym) were incubated in 12-well plates each with 2000 µL of culture medium with approximately 12×10^4 cells for the period of 24 h (in standard conditions). After that time, the medium was removed, cells were rinsed with a phosphate buffer, and a mixture of ethidium bromide (20 µL), calcein (3 µL) was added. The incubation with dyes lasted 30 min. After that time, the surfaces of the samples were observed with the use of fluorescence microscopy (Olympus GX71, Tokyo, Japan). For each sample, 5 photos were taken at various random locations. The number of cells (green: live; red: dead) was calculated. This study was performed in 2 repetitions.

3. Results

3.1. Microscopic Examination

Figure 2 shows the surfaces of the samples produced by 3D printing with and without modifications. In all cases, the applied coating was visible despite significant surface irregularities. The presence of curcumin in sample Cur was easily observed by the yellow color of the coating. The change in the intensity of that color showed an uneven thickness of the film; thicker groves formed after printing.

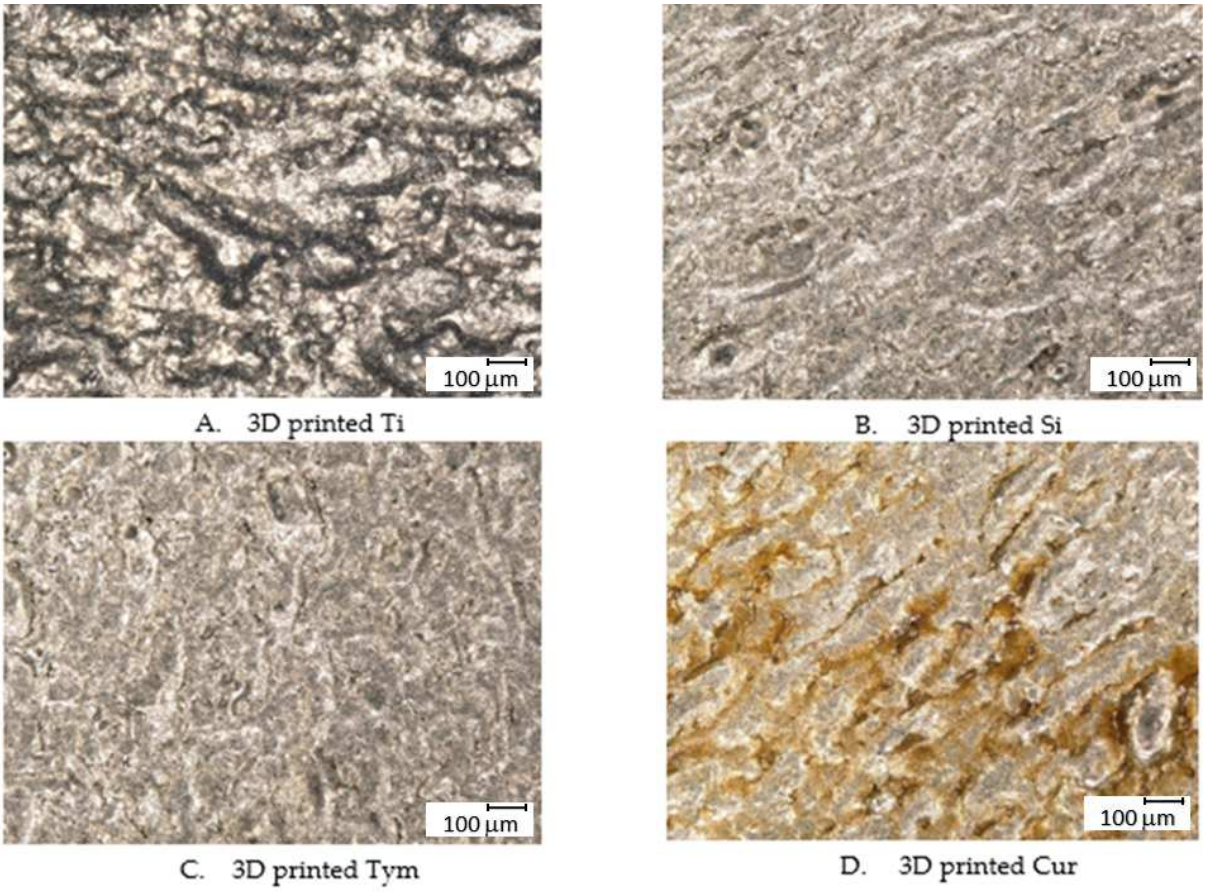


Figure 2. Surfaces of examined 3D-printed samples visualized by means of optical microscopy.

For better visualization of the coatings, the deposition was also performed on mirror-like polished samples (see Figure 3). No cracks or points of delamination were visible. Nevertheless, for the samples with coatings, there were some visible points of distortions and inclusions. In the case of the SiO_2-coated samples (Si), these may have originated from the partial gelation of the sol before its application. For other coatings, this may have been the result of processes common for SiO_2-coated samples and the incomplete dissolution of the natural additives.

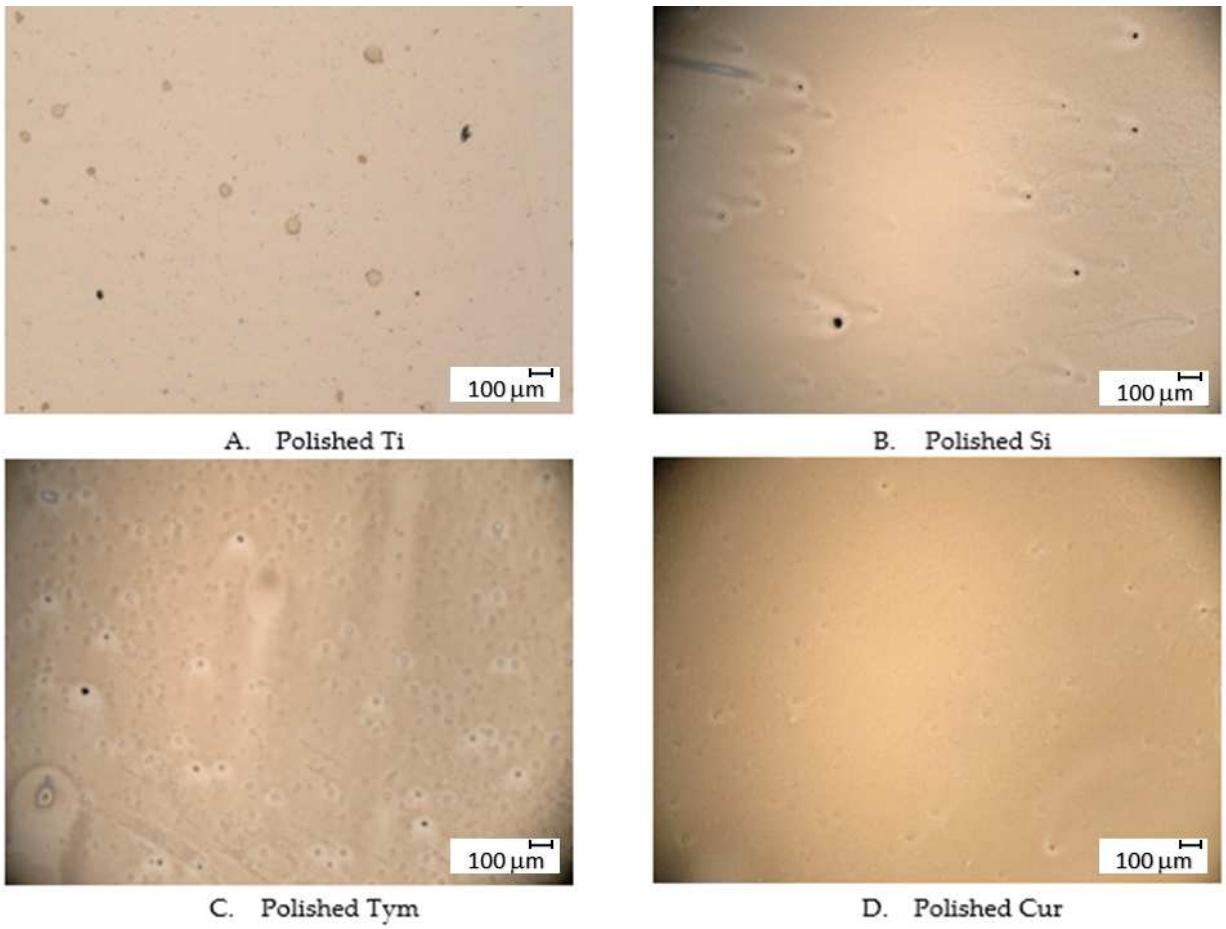


Figure 3. Surfaces of examined mirror-like polished samples visualized by means of optical microscopy.

SEM images of the coatings on printouts are shown in Figure 4. Especially on the surface of the untreated samples, there were visible surface patterning and powder residues after the SLS process. A portion of the used powder was loosely attached and visible as spherical particles on the surface. However, in the case of samples with coatings, those structures were covered with deposited films.

The presence of coatings was also evidenced by the chemical composition of the analyzed surfaces. Table 1 shows the percentage of the silicon content of the examined samples. As expected, the Ti sample did not contain silicon. The contents of this element were different for the Si, Cur, and Tym samples, probably due to differences in the thickness of the coatings.

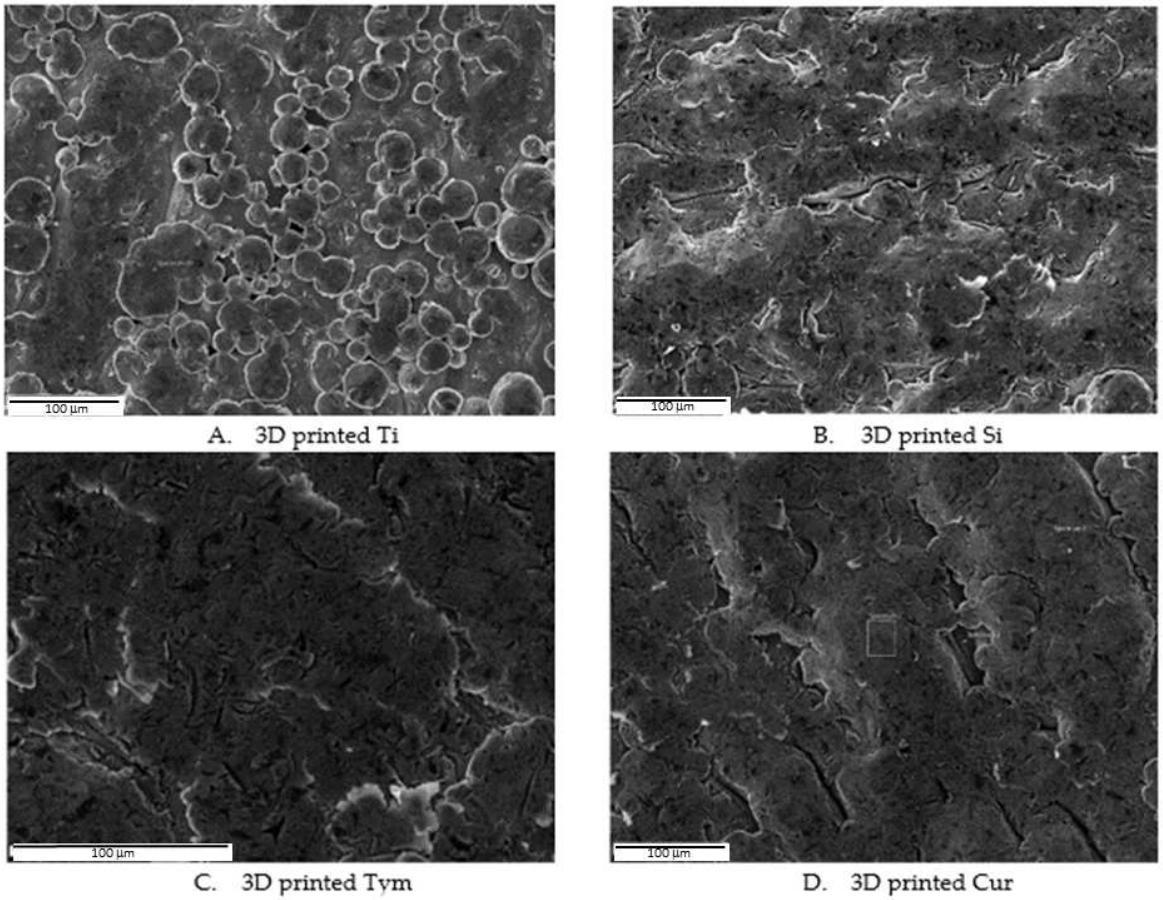


Figure 4. Surfaces of examined 3D-printed samples visualized by SEM.

Table 1. Silicon content in examined printouts obtained with the use of SEM-EDS.

Sample Abbreviation	Ti	Si	Cur	Tym
Silicon content [%]	0.00 ± 0.01	1.36 ± 0.20	1.72 ± 0.17	2.82 ± 0.35

3.2. Surface Roughness and Thickness of Coatings

An increase in roughness was visible for the coatings with added thymol (see Figure 5). That modification led to an over 2.6 rise in the Rz value and a two-times-higher Ra. In the case of Cur, a small increase in the value of Rz was visible but it was on the margin of the marked measurement error. The roughness of Ti and Si was similar.

In order to make an estimate of the coating thickness and determine the effect of additives, the thickness of the coatings deposited on the silicon wafers was measured. The thicknesses of the coatings deposited on the silicon wafers were similar for all produced coatings and amounted to 46 ± 5 nm. It was assumed that the thickness of the coatings produced on 3D printouts was higher due to the roughness of the substrate, but the addition of active agents did not affect their thickness.

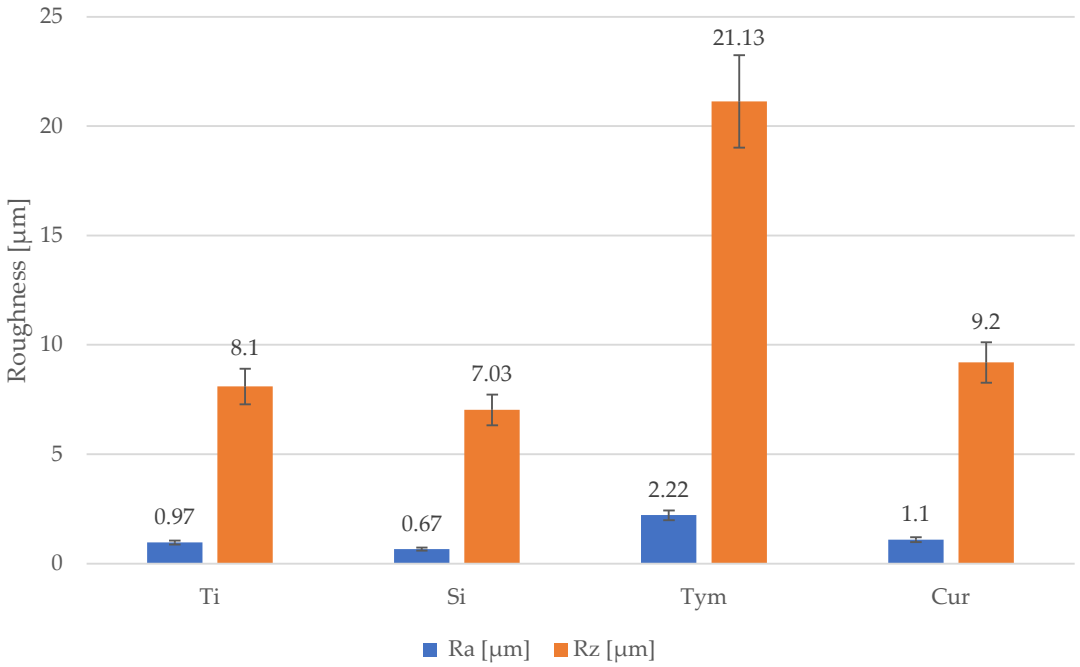


Figure 5. Summary of the roughness of examined 3D-printed surfaces.

3.3. Assessment of Antibacterial Properties

Data on the percentage of live and dead bacterial cells after 10 min and 60 min of incubation are presented in Figures 6 and 7, respectively. Regardless of the coatings' composition, the percentage of dead bacteria increased after 60 min of exposure in comparison to that of the untreated sample. For the 10 min exposure, such a trend was not visible for Tym. In fact, that modification in the mentioned conditions led to almost no dead bacteria. With the increase in the exposure time, the number of dead cells also rose. That change was not visible only for the Si sample. The highest limitation of living microbes was visible for the Cur sample after 60 min of exposure. In that case, almost one-third of the bacteria were dead.

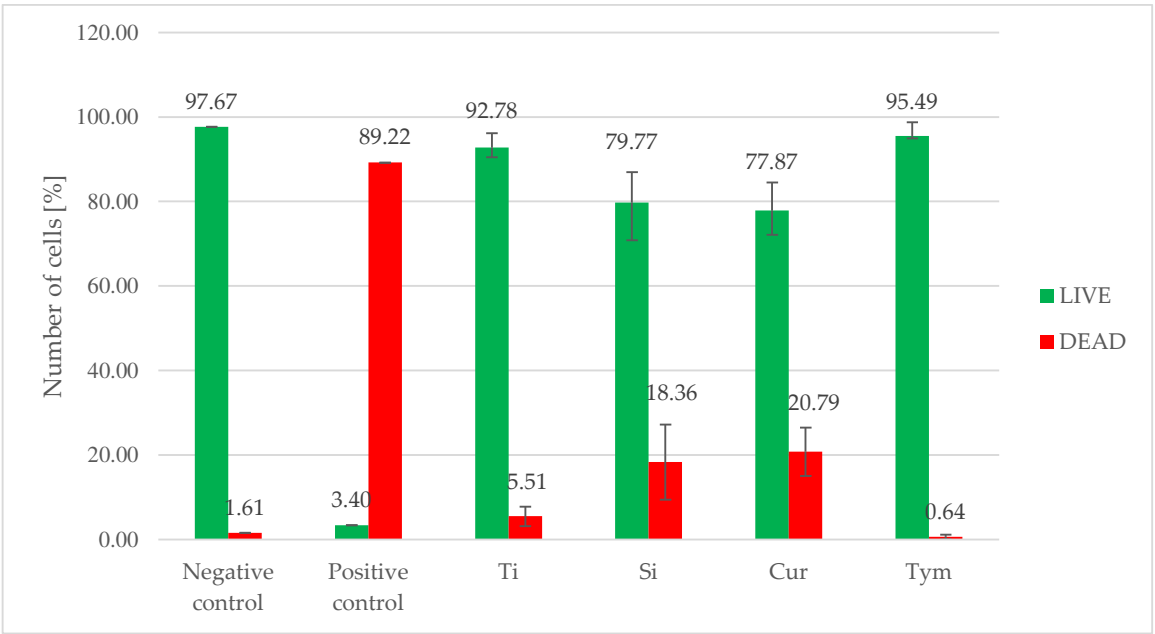


Figure 6. Percentage of live and dead bacterial cells after 10 min of exposure to the tested surfaces.

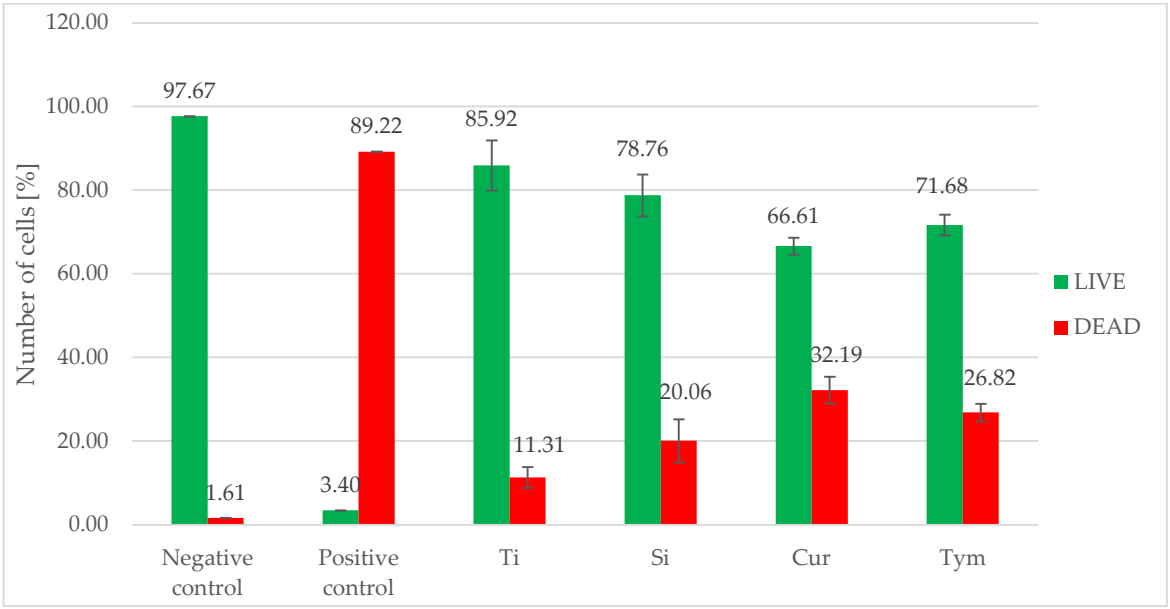


Figure 7. Percentage of live and dead bacterial cells after 60 min of exposure to the tested surfaces.

3.4. Assessment of Cytotoxicity

Figure 8 shows the percentages of the proliferation of Saos-2 cells on the examined surfaces. For all the examined materials, the mean proliferation was no lower than 90%. However, it should be noted that proliferation shows the tendency and ability of cells to reproduce and does not directly provide their amount. Among the modified materials, the largest number of cells was present on the Tym sample (see Figure 9). The total mean value (the sum of live and dead cells) for that type of sample was only slightly lower than the number of cells on the Ti sample (219.2 and 222.6, respectively), but the number of dead cells was almost three times higher (reaching 22.1 and 7.6, respectively). In the case of the printout with the sol-gel coating without any additive, the mean total value of cells was about 20% lower. On the surface of the Cur sample, there was the lowest number of cells, over 50% less than in any of the other cases. The number of dead cells on the Ti, Si, and Cur samples was, in each case, close to 10.

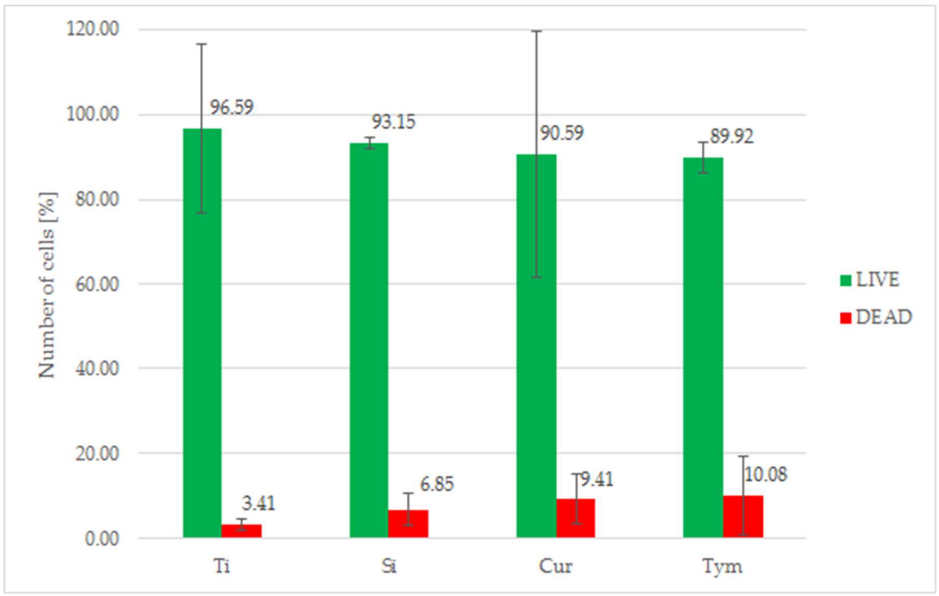


Figure 8. Evaluation of cell proliferation of Saos-2 cell line on examined surfaces.

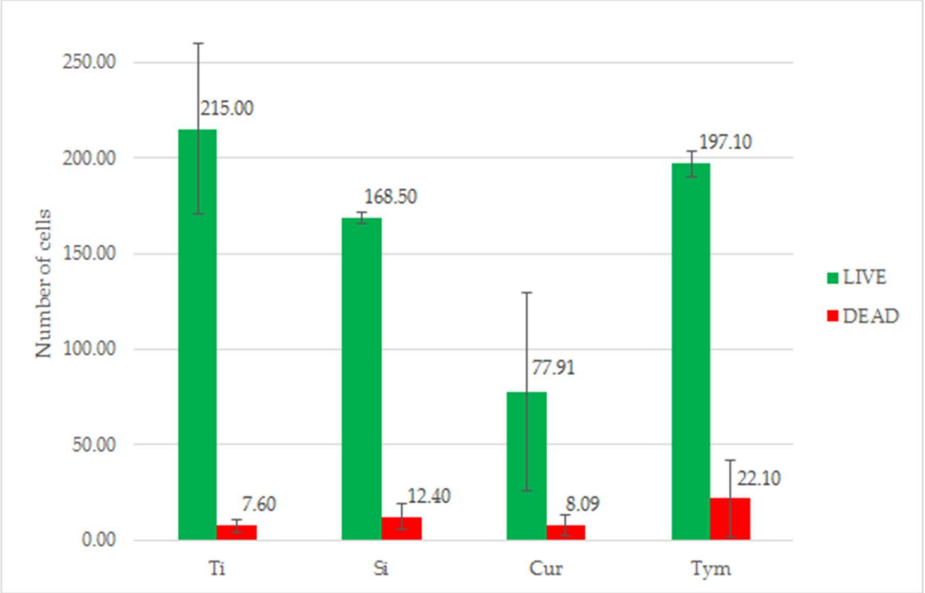


Figure 9. Number of Sos-2 cells on examined surfaces.

4. Discussion

Although only the Cur coating on the 3D printouts allowed the visual assessment of its uneven thickness, it can be assumed that a similar situation also occurs for Si and Tym. Nevertheless, the lack of cracks and signs of delamination proves the successful formation of sol-gel coatings on the samples manufactured by the SLS method. The main application of the proposed coating is not related to increasing corrosion resistance but rather to affecting microbial colonization. It means that even in the case of the discontinuation of the film, the release of natural substances to the surrounding environment is secured, and this reduces the amount of bacteria, as shown by the results of flow cytometry. The 3D printouts did not undergo any postprocessing to remove the loosely bound particles of powder after SLS. Nevertheless, due to the deposition of coatings, the remaining spheres were firmly covered, which may, to some extent, have prevented their detachment from the surface. The presented increase in surface roughness, especially for Tym, was not observed on either optical or SEM, which provided information about the smoothening of the surface. The Ra and Rz parameters may have been affected by the previously mentioned inclusions related to the incomplete dissolution of the additives or sol gelation prior to deposition. An increase in the surface roughness may promote bacterial adhesion to the surface of a material [23]. However, a threshold value that would clearly correspond to the increase in biofilm formation has not yet been established. In the case of the Tym coating, an increase in dead bacteria was still visible.

The results of the bactericidal assessment using flow cytometry did not show a clear bactericidal effect since the portion of dead bacterial cells was not higher than that of the living ones. However, the introduction of thymol and curcumin had a bacteriostatic effect, proved by the significant reduction in living bacteria. Even in the case of the SiO_2 coating without additives, some positive effect on the reduction in bacterial colonization was present. The literature has already described antibacterial properties due to the addition of curcumin [31,34] or thymol [32,33] but with higher contents of these additives. In this study, a low content of the natural agents was selected so as not to affect gelation in the process of the coating deposition. Eventually, the additives of natural agents may have had some effect on the coatings' morphology since their inclusion was present in the Tym and Cur samples. The increase in the number of dead *E. coli* after prolonging the exposure suggests that the antibacterial effect requires the release of the active substance from the coating over time, especially since this effect was stronger for doped films.

The results of the LIVE/DEAD cytotoxicity assessment prove that sol-gel SiO_2-based coatings do not have a cytotoxic effect on Saos-2 cells regardless of their composition. This means that the orthopedic application of such films has no drawbacks concerns surrounding the bone tissue response.

5. Conclusions

Silica sol-gel coatings with natural additives were successfully deposited on 3D printouts made of Ti6Al4V ELI. The addition of both curcumin and thymol led to a bactericidal effect of the synthetized films that is promising for the medical application of such materials and the further use of natural compounds to fight microbial infections. The potential of sol-gel coatings on 3D printouts manufactured in a manner resembling the production of individual implants also had no adverse effect on osteoblasts. The additional advantage of the proposed solution is the covering of loosely attached powders remaining after printing, which may be treated as postprocessing of such printouts. Further studies concerning both a wider range of curcumin and thymol concentrations as well as the evaluation of the durability of the coating are required.

Author Contributions: Conceptualization, N.S., K.C., P.Ł., P.Ś., and L.C; investigation, N.S., K.C., P.Ł., P.Ś., and L.C.; methodology N.S., K.C., P.Ł., P.Ś., and L.C.; supervision, B.P. and K.J.; writing—original draft, N.S., K.C., P.Ł., P.Ś., and L.C.; writing—review and editing, K.J. and B.P. All authors have read and agreed to the published version of the manuscript.

Funding: This research received no external funding.

Institutional Review Board Statement: Not applicable.

Informed Consent Statement: Not applicable.

Data Availability Statement: Data are contained within this article.

Acknowledgments: The authors are thankful for the involvement and support of the members of the Institute of Materials Science and Engineering at the Lodz University of Technology, Witold Jakubowski, Marta Kamińska, Anna Jędrzejczak, and Marcin Makówka in conducting this study. Gratitude is also expressed to Medgal Ltd. for preparing the samples.

Conflicts of Interest: The authors declare no conflicts of interest.

References

1. World Health Organization. Antimicrobial Resistance. 2023. Available online: https://www.who.int/news-room/fact-sheets/detail/antimicrobial-resistance (accessed on 3 May 2024).
2. Jonas, O.B.; Irwin, A.; Berthe, F.C.J.; Le Gall, F.G.; Marquez, P.V. *Drug-Resistant Infections: A Threat to Our Economic Future*; World Bank: Washington, DC, USA, 2017; Volume 2.
3. Slavin, Y.N.; Asnis, J.; Häfeli, U.O.; Bach, H. Metal Nanoparticles: Understanding the Mechanisms behind Antibacterial Activity. *J. Nanobiotechnol.* **2017**, *15*, 65. [CrossRef] [PubMed]
4. Godoy-Gallardo, M.; Eckhard, U.; Delgado, L.M.; de Roo Puente, Y.J.D.; Hoyos-Nogués, M.; Gil, F.J.; Perez, R.A. Antibacterial Approaches in Tissue Engineering Using Metal Ions and Nanoparticles: From Mechanisms to Applications. *Bioact. Mater.* **2021**, *6*, 4470–4490. [CrossRef] [PubMed]
5. Pokrowiecki, R.; Tyski, S.; Zaleska, M. Problematyka Zakażeń Okołowszczepowych. *Postep. Mikrobiol.* **2014**, *53*, 123–134.
6. Cornejo-Juárez, P.; Vilar-Compte, D.; Pérez-Jiménez, C.; Ñamendys-Silva, S.A.; Sandoval-Hernández, S.; Volkow-Fernández, P. The Impact of Hospital-Acquired Infections with Multidrug-Resistant Bacteria in an Oncology Intensive Care Unit. *Int. J. Infect. Dis.* **2015**, *31*, 31–34. [CrossRef]
7. Martina, P.F.; Martinez, M.; Centeno, C.K.; Von Specht, M.; Ferreras, J. Dangerous Passengers: Multidrug-Resistant Bacteria on Hands and Mobile Phones. *J. Prev. Med. Hyg.* **2019**, *60*, E293–E299. [CrossRef] [PubMed]
8. Glajzner, P. Infections Associated with Healthcare—A Still Serious Problem of Healthcare in Poland. *Farm. Pol.* **2019**, *75*, 148–156. [CrossRef] [PubMed]
9. Caselli, E. Hygiene: Microbial Strategies to Reduce Pathogens and Drug Resistance in Clinical Settings. *Microb. Biotechnol.* **2017**, *10*, 1079–1083. [CrossRef]
10. Silver, S.; Phung, L.T.; Silver, G. Silver as Biocides in Burn and Wound Dressings and Bacterial Resistance to Silver Compounds. *J. Ind. Microbiol. Biotechnol.* **2006**, *33*, 627–634. [CrossRef]

11. Lin, W.P.; Huang, Y.S.; Wang, J.T.; Chen, Y.C.; Chang, S.C. Prevalence of and Risk Factor for Community-Onset Third-Generation Cephalosporin-Resistant Escherichia Coli Bacteremia at a Medical Center in Taiwan. *BMC Infect. Dis.* **2019**, *19*, 245. [CrossRef]
12. Gramundi, I.; Albornoz, E.; Boutureira, M.; Rapoport, M.; Gomez, S.; Corso, A.; Castro, G.; Faccone, D. Characterization of Third Generation Cephalosporin-Resistant Escherichia Coli Clinical Isolates from Ushuaia, Argentina. *Rev. Argent. Microbiol.* **2023**, *55*, 43–48. [CrossRef]
13. Kourtis, A.P.; Sheriff, E.A.; Weiner-Lastinger, L.M.; Elmore, K.; Preston, L.E.; Dudeck, M.; McDonald, L.C. Antibiotic Multidrug Resistance of Escherichia Coli Causing Device- and Procedure-Related Infections in the United States Reported to the National Healthcare Safety Network, 2013–2017. Clin. *Infect. Dis.* **2021**, *73*, e4552–e4559. [CrossRef]
14. Centers for Disease Control and Prevention. *Antibiotic Resistance Threats in the United States*; U.S. Department of Health and Human Services, CDC: Atlanta, GA, USA, 2019.
15. Rai, M.; Deshmukh, S.D.; Ingle, A.P.; Gupta, I.R.; Galdiero, M.; Galdiero, S. Metal Nanoparticles: The Protective Nanoshield Against Virus Infection. *Crit. Rev. Microbiol.* **2016**, *42*, 46–56. [CrossRef]
16. Kumah, E.A.; Fopa, R.D.; Harati, S.; Boadu, P.; Zohoori, F.V.; Pak, T. Human and Environmental Impacts of Nanoparticles: A Scoping Review of the Current Literature. *BMC Public. Health* **2023**, *23*, 1059. [CrossRef] [PubMed]
17. Walkowiak, B.; Walkowiak-Przybyło, M.; Komorowski, P. *Biological Evaluation of Materials*; IOP Publishing: Bristol, UK, 2022.
18. Taghavi, S.M.; Momenpour, M.; Azarian, M.; Ahmadian, M.; Souri, F.; Taghavi, S.A.; Sadeghain, M.; Karchani, M. Effects of Nanoparticles on the Environment and Outdoor Workplaces. *Electron. Physician* **2013**, *5*, 706–712. [CrossRef]
19. Hosny, A.E.D.M.S.; Rasmy, S.A.; Aboul-Magd, D.S.; Kashef, M.T.; El-Bazza, Z.E. The Increasing Threat of Silver-Resistance in Clinical Isolates from Wounds and Burns. *Infect. Drug Resist.* **2019**, *12*, 1985–2001. [CrossRef] [PubMed]
20. Cegielska-Radziejewska, R.; Leśnierowski, G.; Kijowski, J. Properties and Application of Egg White Lysozyme and Its Modified Preparations—A Review. *Pol. J. Food Nutr. Sci.* **2008**, *58*, 5–10.
21. Bing, W.; Cai, Y.; Jin, H.; Tian, L.; Tian, L.; Yin, Y.; Teng, Y.; Wang, P.; Hou, Z.; Bai, X. An Antiadhesion and Antibacterial Platform Based on Parylene F Coatings. *Prog. Org. Coat.* **2021**, *151*, 106021. [CrossRef]
22. Ao, H.; Yang, S.; Nie, B.; Fan, Q.; Zhang, Q.; Zong, J.; Guo, S.; Zheng, X.; Tang, T. Improved Antibacterial Properties of Collagen I/Hyaluronic Acid/Quaternized Chitosan Multilayer Modified Titanium Coatings with Both Contact-Killing and Release-Killing Functions. *J. Mater. Chem. B* **2019**, *7*, 1951–1961. [CrossRef]
23. Mu, M.; Wang, X.; Taylor, M.; Castillo, A.; Cisneros-Zevallos, L.; Akbulut, M.; Min, Y.; Akbulut, Y. Min, Multifunctional coatings for mitigating bac-terial fouling and contamination. *Colloid Interface Sci. Commun.* **2023**, *55*, 100717. [CrossRef]
24. Jin, G.; Qin, H.; Cao, H.; Qian, S.; Zhao, Y.; Peng, X.; Zhang, X.; Liu, X.; Chu, P.K. Synergistic Effects of Dual Zn/Ag Ion Implantation in Osteogenic Activity and Antibacterial Ability of Titanium. *Biomaterials* **2014**, *35*, 7699–7713. [CrossRef]
25. Cao, H.; Liu, X.; Meng, F.; Chu, P.K. Biological Actions of Silver Nanoparticles Embedded in Titanium Controlled by Micro-Galvanic Effects. *Biomaterials* **2011**, *32*, 693–705. [CrossRef] [PubMed]
26. Haufe, H.; Muschter, K.; Siegert, J.; Böttcher, H. Bioactive Textiles by Sol–Gel Immobilised Natural Active Agents. *J. Sol-Gel Sci. Technol.* **2008**, *45*, 97–101. [CrossRef]
27. Birkett, M.; Zia, A.W.; Devarajan, D.K.; Soni; Panayiotidis, M.I.; Joyce, T.J.; Tambuwala, M.M.; Serrano-Aroca, A. Multi-Functional Bioactive Silver- and Copper-Doped Diamond-Like Carbon Coatings for Medical Implants. *Acta Biomater.* **2023**, *167*, 54–68. [CrossRef]
28. Molina, J.; Valero-Gómez, A.; Pocoví-Martínez, S.; Ibiza-Palacios, M.S.; Bosch, F. Simple and Effective Sol-Gel Methodology to Obtain a Bactericidal Coating for Prostheses. *J. Sol-Gel Sci. Technol.* **2023**, *108*, 809–826. [CrossRef]
29. Stan, D.; Enciu, A.M.; Mateescu, A.L.; Ion, A.C.; Brezeanu, A.C.; Stan, D.; Tanase, C. Natural Compounds With Antimicrobial and Antiviral Effect and Nanocarriers Used for Their Transportation. *Front. Pharmacol.* **2021**, *12*, 723233. [CrossRef]
30. Chouhan, S.; Sharma, K.; Guleria, S. Antimicrobial Activity of Some Essential Oils—Present Status and Future Perspectives. *Medicines* **2017**, *4*, 58. [CrossRef] [PubMed]
31. Zheng, D.; Huang, C.; Huang, H.; Zhao, Y.; Khan, M.R.U.; Zhao, H.; Huang, L. Antibacterial Mechanism of Curcumin: A Review. *Chem. Biodivers.* **2020**, *17*, e2000171. [CrossRef]
32. Nagoor Meeran, M.F.; Javed, H.; Al Taee, H.; Azimullah, S.; Ojha, S.K. Pharmacological Properties and Molecular Mechanisms of Thymol: Prospects for Its Therapeutic Potential and Pharmaceutical Development. *Front. Pharmacol.* **2017**, *8*, 380. [CrossRef]
33. Kowalczyk, A.; Przychodna, M.; Sopata, S.; Bodalska, A.; Fecka, I. Thymol and Thyme Essential Oil—New Insights into Selected Therapeutic Applications. *Molecules* **2020**, *25*, 4125. [CrossRef]
34. Raduly, F.M.; Rădiţoiu, V.; Rădiţoiu, A.; Frone, A.N.; Nicolae, C.A.; Purcar, V.; Ispas, G.; Constantin, M.; Răut, I. Modeling the properties of curcumin derivatives in relation to the architecture of the siloxane host matrices. *Materials* **2021**, *15*, 267. [CrossRef]
35. Irizar, P.; Pintor-Rial, A.; Martinez-Arkarazo, I.; Olazabal, M.A.; Ruiz-Rubio, L.; Cardiano, P.; Gomez-Laserna, O. Bio-based hybrid nanocomposites as multifunctional sustainable materials for stone conservation. *Prog. Org. Coat.* **2023**, *185*, 107899. [CrossRef]
36. *ISO PN-EN 10993-5*; Biological evaluation of medical devices—Part 5: In vitro cytotoxicity tests. International Standard Organization: Geneva, Switzerland, 2009.

Disclaimer/Publisher's Note: The statements, opinions and data contained in all publications are solely those of the individual author(s) and contributor(s) and not of MDPI and/or the editor(s). MDPI and/or the editor(s) disclaim responsibility for any injury to people or property resulting from any ideas, methods, instructions or products referred to in the content.